

DYNAMIC MODELLING OF A NANOMANIPULATOR CHAIN

Ondřej Jež^{*,1} Alina Voda-Besançon^{**}
Sylvain Marlière^{***} Gildas Besançon^{****}

** Dept. of Control and Instrumentation, FEEC, Brno
University of Technology, Kolejní 4, CZ-612 00 Brno,
Czech Republic*

*** Laboratoire d'Automatique de Grenoble INPG /
ENSIEG BP46, 38402 St Martin d'He'eres - Cedex, France*

**** Laboratoire ICA-ACROE, INPG, 46 av. Flix Viallet,
38 031 Grenoble Cedex, France*

***** Laboratoire d'Automatique de Grenoble INPG /
ENSIEG BP46, 38402 St Martin d'He'eres - Cedex, France*

Abstract: This paper presents a dynamic system modelling approach of a nanomanipulator chain developed by the ICA-ACROE and LEPES laboratories. The chain is a very complex instrument, serving for precise sensing and manipulation in nanometer scale environment. The objective is to find a suitable model of the chain in view of stability and performances analysis, and for further control design of the feedback loops. Such a global model is here developed using state space representation of the different parts of the chain. Moreover, an experimental modelling and identification of the cantilever parameters are presented. The nanoscale tip-sample interaction forces are modelled too. Finally the simulation of the whole nanomanipulation chain is performed, simulating the approach-withdrawal operation which is in good accordance with the real patterns of experiments in physics. *Copyright*©2005 IFAC

Keywords: nanosystems, instrumentation, force and position control, modelling, force feedback

1. INTRODUCTION

With the recent development of technologies for precise sensing and manipulation, the nanotechnologies became an emerging issue in many scientific fields like biology, physics, instrumentation etc. Today's nanotechnologies focus on sensing and manipulation capabilities in nano-space, which would in their applications allow us to act directly on living systems or physical structures

with sofar unreached precision. This trend is also influencing the robotics field, whose scientists are trying to develop reliable tools for nanomanipulation and sensing.

This study is focusing on teleoperated nanoscale manipulation and sensing system, developed in the ICA-ACROE and LEPES laboratories, a tool that is allowing a human gestural interaction with a nanometer scale environment through a virtual environment. The term "teleoperation" implies the existence of certain distance between the operator's environment and the environment with

¹ Most of this work was achieved during my training period in Laboratoire ICA-ACROE, Grenoble - France.

which he interacts. This distance is appearing especially in the scale and in the dynamics. While the distance in scale is obvious, the dynamics distance is determined by the physical laws: in the nanometer scale, the surface and adhesion forces dominate the inertial forces whereas in the macro-environment, we usually experience the opposite. One instrumental way to ease the complications raising from this phenomenon is the creation of a new environment, which serves as the median between the two distant environments. This is realized by creating a mixed (augmented) reality, where the real nanometer scale environment and the real user's macro-scale environment interact.

Yet another extension to the augmented reality is being developed. It is the PC control system that is connected to the main workstation, which also contains an ethernet connection allowing internet utilization. Such extension will allow distant monitoring, visualisation, and control from everywhere, creating global research groups either in industry or in academic area. The distant PC control will make the present nanomanipulator a lot more flexible instrument.

The objective of this paper is to describe and identify different parts of the nanomanipulator system developed by ICA-ACROE/LEPES laboratories, find models of these parts and also describe them in the state space representation. The chain has so far been described only with the *cordis anima* modelling approach, which was also proposed in the ICA-ACROE laboratory. It is now necessary to obtain a simulation scheme, which can be further used for simulations.

The motivation of system approach - modelling and finding state space representations - is following: the simulation of the behavior of the nanomanipulation chain will allow testing of the device under different conditions avoiding any damage on samples or the device itself. Tuning the parameters of the models during the simulation can help to find optimal setting of the chain parameters with respect to the desired function. The model and state space representation can serve further for stability and dynamics analysis of the device.

A simple scheme of the nanomanipulator is shown in fig. 1. A more detailed block diagram follows in fig. 2. The main parts of the chain are the following: Force Feedback Gestural Device (FFGD) serving for human control, Atomic Force Microscope (AFM) for sensing and manipulating in nano-scale environment, Real Time Workstation (RTWS) for the function described above. Yet another device is the Electronic Virtual Mass board, which was developed for interconnection purposes between AFM and RTWS. All specific parts of the chain will be studied in detail, presenting their functions and principles accompanied by models

and, where possible, by state space representation. Simulations will be also performed.

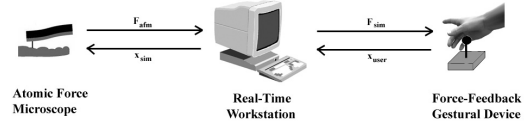


Fig. 1. The main operational principle of the nanaomanipulator

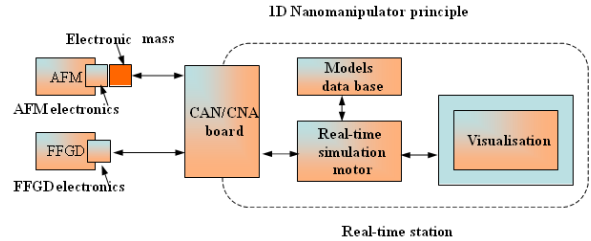


Fig. 2. A more detailed block diagram of the nanomanipulator

2. ATOMIC FORCE MICROSCOPE

The Atomic Force Microscope (further AFM) works on the principle of scanning the environment with a probe with a sharp tip and therefore it is also often called a Scanning Probe Microscope. The AFM is designed for exploration and modification of object surfaces in nanometer scale.

Most AFMs utilize cantilever-type probes. A typical cantilever is shown in fig. 3. The tip of the cantilever interacts with the nano-scale world and as forces are exerted on it, its lever bends and creates a deflection of the tip from the base position.

To sense the tip's deflection, most AFM's have a laser generator and a photodetector system. The laser shines on the tip which reflects the beam to the photo detector. As the tip moves up and down, the reflected beam also changes its position on the photodetector and that results in changes in photo detector's output. The cantilever is mounted on a piezo drive, which is able to provide positioning of the cantilever with a very high precision. The resolution of such actuator usually goes down to tenths of nanometer or even lower if used in open loop.

The nanomanipulator uses the AFM in contact mode. Then the cantilever can be modelled as a simple mechanical oscillator - a system of a mass attached through a spring and a damper to the piezo drive. This is illustrated in fig. 3.

There are three unknown parameters of such model: spring constant k_{can} , damping constant

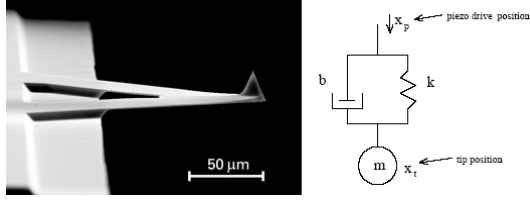


Fig. 3. Mechanical model of a cantilever type probe

b_{can} and the mass of the tip m_{tip} . Please note that the mass of the tip just a modelled mass, it is not a real tip mass, because in the cantilever the mass is distributed through its length.

The model of the AFM will be further reduced to the model of the cantilever. This is mainly because the reception principle is difficult to model and also because in the manipulator we bypass most of the electronics that are normally used in the operation of the AFM. The simulation scheme (block model) of the cantilever is shown in fig. 4. The model has been obtained using bond graph method. A corresponding state space representation of the classical form $dz/dt = Az + Bu$, $y = Cz + Du$, with input u and output y , can be given by matrices 1 to 3 below.

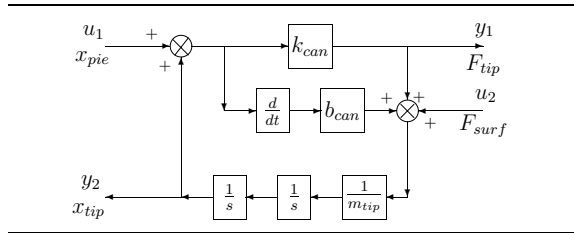


Fig. 4. Simulation scheme of a cantilever type probe

$$\mathbf{A} = \begin{pmatrix} 0 & 1 \\ -\frac{k_{can}}{m_{tip}} & -\frac{b_{can}}{m_{tip}} \end{pmatrix} \quad (1)$$

$$\mathbf{B} = \begin{pmatrix} \frac{b_{can}}{m_{tip}} & 0 \\ \frac{b_{can}^2}{m_{tip}^2} + \frac{k_{can}}{m_{tip}} & \frac{1}{m_{tip}} \end{pmatrix} \quad (2)$$

$$\mathbf{C} = \begin{pmatrix} k_{can} & 0 \\ 1 & 0 \end{pmatrix} \quad \mathbf{D} = \begin{pmatrix} k_{can} & 0 \\ 0 & 0 \end{pmatrix} \quad (3)$$

Although the parameters of the cantilever were specified by the manufacturer, due to their high tolerances, some parameter identification was required. The first (and the easiest) task is to determine the resonant frequency of the cantilever. One way to measure the frequency characteristics of the cantilever is simply to measure and analyze the output without exciting the piezo. This is possible because the cantilevers are usually so sen-

sitive, that they react to the thermal noise (brownian motion), whose characteristics are similar to the characteristics of the white noise. This analysis was performed and its results also confirmed by exciting the cantilever with a sweep sinusoid signal. The first resonance mode frequency of the cantilever was measured at 24300 Hz.

One way to compute the spring constant from the geometrical properties of the cantilever is proposed in (Sarid, 1994). His example uses a rectangular lever, but according to (Gibson et al., 1996), our V-shaped cantilever can be approximated by two rectangular beams in parallel, or, by one beam of a double width. The equation of such calculation is given in 4, where L is the length of the cantilever, E is the elastic modulus of the material (for silicon typically 135MPa), w is the cantilever's width and t is the thickness of the cantilever. But here we get to the problem of uncertain thickness t of the cantilever, which varies from $0.7\mu m$ to $1.3\mu m$. But according to (Sarid, 1994), the relation between the resonance frequency ω_r and the thickness t is 5, where m_c is a concentrated mass of the cantilever and m_d is its distributed mass. For our cantilever and for the first (and fundamental) resonance frequency, the m_c is close to zero. Therefore the interdependence of ω and t could be approximated with a linear function. This function was determined from manufacturer's specifications (taking into account material constants etc.) Solving this function for our resonance frequency, we got thickness $t = 0.85\mu m$, using this value in 4, where $E=135MPa$, width of the cantilever is $w = 80\mu m$ (two $40\mu m$ beams) and its length is $L = 200\mu m$, we get $k_{can} = 0.21Nm^{-1}$.

$$k_{can} = \frac{Ewt^3}{4L^3} = 0.21Nm^{-1} \quad (4)$$

$$\omega_r = \sqrt{\frac{Ewt^3}{4L^3(m_c + 0.24wtL\rho)}} \approx t\sqrt{\frac{E}{0.96L^4t\rho}} \quad (5)$$

The mass of the modelled oscillator was obtained from k_{can} , f_r using equation 6. The damping constant $b_{can} = 2.34 \cdot 10^{-9}$ was determined from the quality factor Q using equation 7, where the $Q = 610$ was measured from the thermal noise excitation frequency characteristic.

$$m_{tip} = \frac{k}{4\pi^2 f_r^2} = 9.7147 \cdot 10^{-12} kg \quad (6)$$

$$b_{can} = \frac{\sqrt{m_{tip}k_{can}}}{Q} = 2.34 \cdot 10^{-9} Nm^{-1}s \quad (7)$$

In order to complete the model of the AFM, surface-interaction model has to be created. In nanometer scale, surface and friction forces dominate the inertial forces, dynamics become faster

etc. In order for this model to match the real systems, all dominant forces have to be modelled. These are mainly van der Waals, capillary and electrostatic forces. All these were modelled and included in the nanomanipulator chain.

The approach-withdrawal simulation is displayed in figure 5. We can see the position of the tip (x_{tip}) and the position of the cantilever drive - piezo (x_{pie}) while the piezo approaches and withdraws from the surface. The snap-on and snap-off of the cantilever tip is clearly visible, as well as the hysteresis - "sticking" - effect caused mainly by capillary forces. We also observe that electrostatic forces (voltage between the tip and the sample is 10V) are causing a low deflection of x_{tip} from x_{pie} at quite long distances (such as 20 to 30nm).

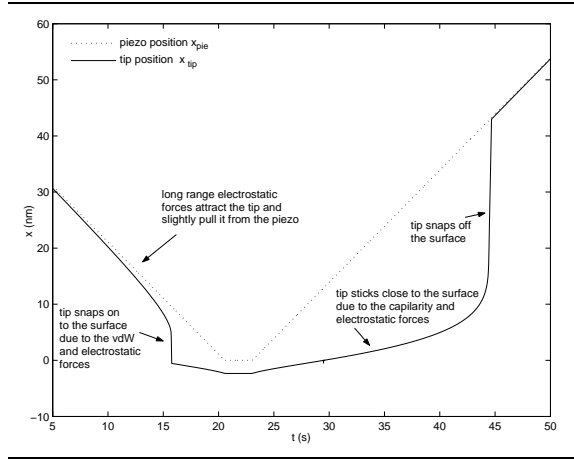


Fig. 5. Approach-withdrawal simulation with vdW, capillary and electrostatic forces

3. ELECTRONIC VIRTUAL MASS

Electronic Virtual Mass board serves as a signal converter between the Atomic Force Microscope and the Real Time Workstation. The problem is that the output of the Atomic Force Microscope is a force signal while its input is a position signal. The Real Time Workstation - Telluris - on the other hand handles force signals as outputs and position signals as inputs. Electronic Virtual Mass therefore converts the force signals into a single position signal, its equivalent mechanical model would be a mass that is attached to the ground by a spring and a damper. The input forces are exerted on this mass and the output signal is its position.

The model of the Electronic Virtual Mass board can be seen in fig. 6. The blocks represent different operation amplifiers with attached resistors and condensers. The parameters will not be presented in this paper, though the setting has been taken from the board while testing the device. This simulation scheme was obtained directly from the

electronic scheme (not presented here) by creating transfer functions of all operational amplifiers. A state space representation can be derived for this model with matrices as follows:

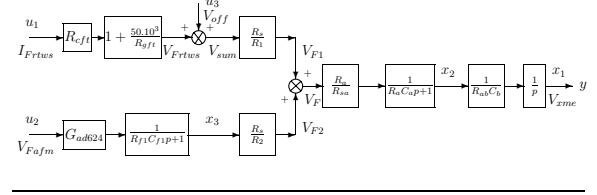


Fig. 6. Detailed simulation scheme of the Electronic Virtual Mass

$$\mathbf{A} = \begin{pmatrix} 0 & \frac{1}{R_{ab}C_b} & 0 \\ 0 & -\frac{1}{R_a C_a} & \frac{R_s}{R_1 R_{sa} C_a} \\ 0 & 0 & -\frac{1}{R_{f1} C_{f1}} \end{pmatrix} \quad (8)$$

$$\mathbf{B} = \begin{pmatrix} 0 & 0 & 0 \\ \frac{(R_{gft} + 50 \cdot 10^3) R_{cft} R_s}{R_1 R_{sa} R_{gft} C_a} & 0 & \frac{R_s}{R_1 R_{sa} C_a} \\ 0 & \frac{G_{ad624}}{R_{f1} C_{f1}} & 0 \end{pmatrix} \quad (9)$$

$$\mathbf{C} = (1 \ 0 \ 0) \quad \mathbf{D} = (0 \ 0 \ 0) \quad (10)$$

4. FORCE FEEDBACK GESTURAL DEVICE

The laboratory ICA-ACROE has a long history in developing the Force Feedback Gestural Devices. In the nanomanipulator, the FFGD serves to the user as a controlling device, which has the capability of force feedback on his/her hand. The native regime of this device in terms of impedance/admittance from the RTWS point of view is the *impedance mode*, since the FFGD converts a force signal (which can be viewed as effort variable) to a position signal (which is in fact flow value). The opposite way - transforming a position signal into a force is called the *admittance mode*, which is currently being developed.

Since the AFM is not a microscope in the classical meaning of the word, but it is in fact a force sensing device, force feedback haptic control is a very suitable option for the nanomanipulator from both control and perception point of view. The force feedback allow user precise mechanical sensing and also more accurate control. The only possible disadvantage - if the force actuated on the user limit him from manipulating - can be minimized in the appropriate setting of the model in RTWS.

The input of the FFGD is a voltage signal from the RTWS corresponding to the force F_{sim} signal. The FFGD interacts with the user by exerting the force F_{tgr} on him. The user in this interaction sets the position of the controller x_{user} , which is measured and sent to the RTWS as the x_{tgr} signal. The range of the amplified input voltage signal from the RTWS is $\pm 5V$. The position range of the FFGD is about $\pm 1.5cm$.

It was also necessary to create a model of the user that is controlling FFGD. The electrical/mechanical scheme of the FFGD and the user is shown in figure 7. The FFGD consists of a differential amplifier, an electrical circuit with its resistance R , a coil with inductance L , reostat R_{reo} for obtaining current value for differential amplification (its maximum value is R_{mreo} , then also of a electromechanical bond converting the current I to the force $F = C_{tgr}I$ exerted on the mass of the FFGD and the user. C_{tgr} is the electromechanical constant of the FFGD. The mass m is attached to the ground by a damper and a spring with constants $b_{us} + b_{tgr}$ and k_{us} . The damper represents the damping performed by the user b_{us} and also the friction of the FFGD mechanism b_{tgr} . The spring corresponds to the fact that user does usually have a desired position in which, as well as a spring, he tries to lead the device. The velocity of the movement v also induces voltage $V = C_{tgr}v$ in the electrical circuit (this is represented by the voltage source). The simulation scheme, obtained using bond graph modelling method, follows in figure 8. C_{lvd} is the constant of the position sensor.

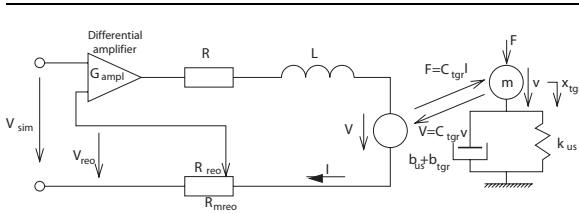


Fig. 7. Mechanical/electrical scheme of the FFGD and the User

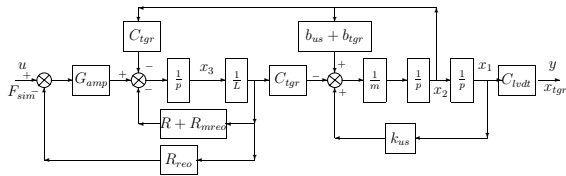


Fig. 8. Simulation scheme of the FFGD and the User

The corresponding state space representation is given by matrices:

$$\mathbf{A} = \begin{pmatrix} 0 & 1 & 0 \\ k_{us} & b_{tot} & -\frac{C_{tgr}}{L} \\ 0 & -C_{tgr} & -\frac{R_{reo}G_{amp} + R + R_{mreo}}{L} \end{pmatrix} \quad (11)$$

$$\mathbf{B} = (0 \ 0 \ G_{ampl}) \quad (12)$$

$$\mathbf{C} = (C_{lvd} \ 0 \ 0) \quad \mathbf{D} = 0 \quad (13)$$

The parameters of the FFGD have been obtained from the schematics of the FFGD and from the creators of the device. The user was set in such way, that if we exert maximum force on him, he would keep the TGR in the range of the output $\pm 1.5cm$. The spring constant is therefore very high $200Ncm^{-1}$, the damping constant of the user is also set quite high $10Nscm^{-1}$ so that the oscillations are damped.

5. REAL TIME WORKSTATION

The Real Time Workstation (RTWS) serves as the interface between the two realities: the nanometer scale world of the cantilever and the macro environment of the human being. It creates a virtual environment, in which it processes the input signal from both realities and lets them interact in a way they can both perceive.

The RTWS is built on the Silicon Graphics Workstations platform, which has been modified in order to overcome the real-time computation constraints, especially the input/output section. The operational system is Unix which allows the separation of one of the machine's four 90 MHz processors solely for the simulation calculations. The modelling language is called Telluris and is a creation of ICA-ACROE laboratory.

The model which is currently being used for the nanomanipulator chain is a simple model of only two masses connected to each other by a spring. The two position inputs of the RTWS determine the position of these masses, while the force the spring exerts on each mass is taken as the output. Due to the simplicity of such model, we will not display it in this paper.

6. NANOMANIPULATOR CHAIN SIMULATIONS

In order to verify the behavior of the whole model, a simulation of the approach-withdrawal operation was performed. In this paper we will present and describe the more interesting - withdrawal part operation. The simulation results are displayed in figure 9. The user's movement was simulated through moving the reference point of the

user's spring to the desired value. This reference position of the spring during withdrawal operation was set to start raising from the surface with rate $+5nm s^{-1}$ at time $t = 14s$.

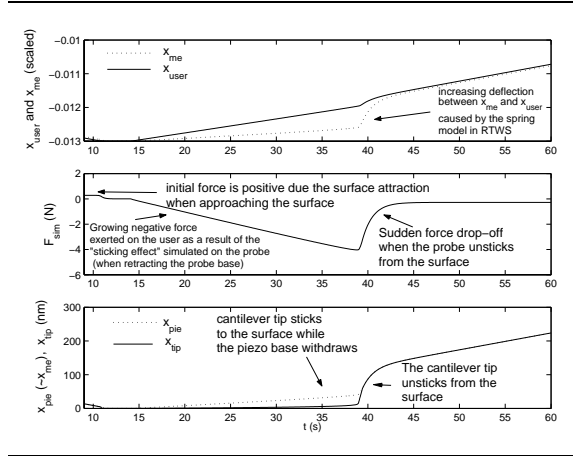


Fig. 9. Withdrawal simulation on the nanomanipulator chain model

In the figure, we can see that the AFM forces can be exerted on the user during the withdrawal movement (see fig. 9). The variables x_{tip} and x_{pie} correspond to the positions of the cantilever tip and probe base (piezo element), F_{sim} is the force exerted on the user and the x_{me} and x_{user} are scaled positions of the user and the virtual - electronic mass. The tip “sticks” to the surface causing a force exerted on the Electronic Virtual Mass. User exerts also a force in the E.V.M. by pulling it up from the surface, though he can actually feel the resistance against this movement (see force F_{sim}). In the time $t = 40s$, the force exerted on E.V.M. from the AFM drops as the tip snaps off the surface, resulting in a sudden drop off in the F_{sim} force exerted on the user. This drop off causes the “released” user to pull up faster for an instant (see x_{user}) and then getting back to the preprogrammed trend in withdrawal.

In this simulation, the phenomenon of the “sticking” effect is simulated and the reaction of the chain model is examined. The user in the chain (in this case represented by a mass, spring and a damper) can observe the phenomenon especially during the withdrawal operation.

7. CONCLUSION

The paper presented and explained the functioning of the nanomanipulator chain developed by ICA-ACROE and LEPES laboratories and also presented models of the devices in the chain as well as their state space representation. The most attention was given to the Atomic Force Microscopy issue, mainly because it is the component in the chain that introduces a distant environment of the nano-scale, whose dynamics

and physical laws differ from the ones we experience. Tip-surface interaction was also modelled using non-linear functions and simulating van der Waals, repulsive, capillary and electrostatic atomic forces. Much attention was also given to the force feedback gestural device, which serves as the transducer between the human-sensible mechanical reality and the virtual space in the workstation. The user was modelled with a second order system.

Bond graphs were chosen as the main modelling method for finding suitable models. This method provides very good results for both mechanical and electrical systems. The models were used for modelling of a basic phenomenon appearing in manipulation in nanometer scale: the hysteresis - “sticking” - effect of the atomic forces actuation during the approach-withdrawal operation of the nanomanipulator’s probe.

Currently, a PC control system with ethernet adapter allowing distant access and control via internet is being developed. Such extension of the manipulator will allow the existence of global scientific projects with flexible real-time distant experimenting, profiting from the scientific potential of many people all over the world.

REFERENCES

- Gibson, T., Watson, G., Myhra, S. (1996): *Determination of The Spring Constants of Probes for Force Microscopy/Spectroscopy*, Journal of Nanotechnology, Vol.7(1996), Institute of Physics Publishing, p. 259-262
- Luciani, A., Marlière, S., Urma, D., Marchi, F., Chevrier, J. (2003): *Approaching Nano-Spaces: 1-DOF Nanomanipulator*, Proceedings of the TNT2003 conference, September 15-19, Salamance - Spain
- Marquis-Favre, W., Scavarda, W. (2002): *Alternative Causality Assignment Procedures in Bond Graph for Mechanical Systems*, Journal of Dynamic Systems, Measurement and Control, Vol. 124 (2002), ASME, p. 457-463
- Nouri, J. (1992): *Etude pour la conception de transducteurs gestuels a retour d'effort et de modeles de systemes mecaniques pour leur controle*, PhD. thesis, INPG, Grenoble-France
- Sarid, D. (1994): *Scanning Force Microscopy With Applications to Electric, Magnetic and Atomic Forces*, Oxford University Press, New York
- Sitti, M., Hashimoto, H. (2003): *Teleoperated Touch Feedback from the Surfaces at the Nanoscale: Modelling and Experiments*, IEEE/ASME Transactions on Mechatronics, Vol.8, No. 1